

THE BOEING COMPANY
Aerospace Group

IDENTIFYING OPTIMUM PARAMETERS OF HOT EXTRUSIONS

Contract NAS 7-276

Prepared for

Chief, Materials Research Branch
National Aeronautics & Space Administration
Headquarters
Washington, D.C.

Progress Report No. 10
16 July 1966 to 18 October 1966

FACILITY FORM 602

N67 12991
(ACCESSION NUMBER)
41
(PAGES)
CR 80365
(NASA CR OR TMX OR AD NUMBER)

1
(CODE)
18
(CATEGORY)

GPO PRICE \$ _____

CFSTI PRICE(S) \$ _____

Hard copy (HC) 2.00

Microfiche (MF) .50

THE BOEING COMPANY
Aerospace Group

IDENTIFYING OPTIMUM PARAMETERS OF HOT EXTRUSIONS

Contract NAS 7-276

Prepared for

Chief, Materials Research Branch
National Aeronautics & Space Administration
Headquarters
Washington, D.C.

Progress Report No. 10
16 July 1966 to 18 October 1966

ABSTRACT

The purpose of this program is to develop a technique for hot extruding MgO and to determine the effect of hot extrusion on MgO and other oxides bodies.

Chemical polishing of extruded MgO was shown to generally not reduce strength if the specimens were first annealed. These results show that strength reduction by chemical polishing found in unannealed MgO extrusions was due to residual stresses.

Strength of extruded MgO fractured parallel to the extrusion axis was shown to be about the same as the strength of hot pressed MgO; substantially less than for extruded MgO fractured perpendicular to the extrusion axis. This provides strong support for the dislocation crack nucleation mechanism in MgO. Evidence of slip bands and internal fractures supporting this mechanism were also found.

It was shown that there is an increasing incidence of surface fracture origins in extruded MgO at both elevated temperatures and room temperature after annealing or chemical polishing. This supports the concept of work hardening of surface MgO grains during grinding and sanding. Direct evidence of such hardening was found.

CONTENTS

	<u>Page</u>
I. WORK ACCOMPLISHED	1
A. EXTRUSION	1
B. MATERIAL ANALYSIS	1
II. DISCUSSION AND CONCLUSION	5
A. MgO	5
B. Al_2O_3	7
III. FUTURE WORK	8
APPENDIX	27

LIST OF FIGURES

<u>Figure No.</u>	<u>Title</u>	<u>Page</u>
1	FURTHER EXAMPLES OF SLIP BANDS AT TRANSVERSE FRACTURE ORIGINS	14
2	ROOM TEMPERATURE STRENGTH OF EXTRUDED MgO	15
3	SAMPLE LONGITUDINAL FRACTURES	16
4	LONGITUDINAL FRACTURE ORIGIN AREA OF M-f-31 ₁₋₁	18
5	2400°F(1315°C) MgO STRENGTH	19
6	FRACTURE ORIGINS OF EXTRUDED FUSED SPECIMENS TESTED AT 2400°F(1315°C)	20
7	2400°F(1315°C) FRACTURE SURFACES OF EXTRUDED HOT PRESSED MgO	21
8	OBJECTS ON EXTRUDED MgO GRAIN BOUNDARY SURFACES	22
9	IR TRANSMISSION OF EXTRUDED MgO	23
10	EXTRUDED Al ₂ O ₃ BILLET A-1-4 IN CAN	24
11	SAMPLE EXTRUDED Al ₂ O ₃ CROSS SECTIONS	25
12	MICROSTRUCTURE OF Al ₂ O ₃ BILLET A-1-4 (COORS AD-99)	26

LIST OF TABLES

<u>Table No.</u>	<u>Title</u>	<u>Page</u>
I	Al ₂ O ₃ EXTRUSION PARAMETERS	9
II	SURFACE FINISH EFFECT ON STRENGTH OF EXTRUDED MgO	10
III	SURFACE FINISH EFFECT ON FRACTURE OF EXTRUDED MgO	11
IV	EFFECT OF SHORT TEST SPANS ON EXTRUDED MgO TRANSVERSE BEND STRENGTH	12
V	Al ₂ O ₃ STRENGTH	13

I. WORK ACCOMPLISHED

A. EXTRUSION

The new, larger, ZrO_2 -insulated induction furnace for heating billets (using the can as a susceptor) has been completed, and successfully checked out and used.

The second extrusion of 1.0 and 1.5" diameter Al_2O_3 billets in a TZM can was successfully performed with an area reduction ratio of 9 to 1 after heating the billet to 1850°C and the catch tube to 1750°C . (See Table I) The front of the extrusion was brought to rest in the catch tube by stalling the tail of the extrusion, as planned. The heated catch tube was maintained at 1650°C (to which it had cooled because power is shut off during extrusion as a safety precaution) for 20 minutes then cooled about $45^\circ\text{C}/\text{minute}$ to 1200°C , then about $35^\circ\text{C}/\text{minute}$ to 1000°C , then removed from the catch tube to cool in the air. The can surface was quite smooth indicating good extrusion conditions.

The first trial of extruding round billets in a round can through a square die was unsuccessful due to an unexplained stall; however, the can and billets may be reusable.

A trial extrusion of MgO-ZrO_2 , MgO-CaO , and $\text{MgO-Al}_2\text{O}_3$ was aborted due to the failure of the billet to drop from the furnace at 2350°C . This was found to be due to melting of the ZrO_2 furnace insulation which is not yet understood. The can and billets appear to be reusable.

B. MATERIAL ANALYSIS

1. MgO Cracking

Successful longitudinal cutting and grinding of a 6-inch-long slab from billet M-3-18 extruded into the heated catch tube (MgO-14) indicates that no transverse fracturing had occurred. No sign of longitudinal cracks were seen in the forward billet. No transverse cracking was found in grinding of a 6.5-inch section of a billet (M-3-9) further back in this extrusion. However, this same section, which did not have as slow cooling, has some longitudinal cracking.

2. MgO Strength and Fracture

(a) Annealing

Further limited analysis of the effect of annealing on strength and fracture is in accord with earlier results showing the same or greater

room temperature strength for specimens annealed at temperatures up to 2800°F(1540°C). Again, there is a generally increasing amount of intergranular fracture with increasing anneal temperature. This intergranular fracture is generally most prevalent on the tensile side of the specimen and is found most frequently in billets made from powder or grain rather than from fused ingots. There also appeared to be an increasing tendency for fracture origins to occur at the surface of specimens tested as annealed.

(b) Effect of Surface Finish

Extruded sections were annealed, then cut and ground to bars which were sanded then broken near one end in 3 point flexure. Then the larger remaining section was chemically polished at least 5 minutes in boiling (about 150°C) phosphoric acid (diluted to a density of about 1.35 gm/cc for better polishing) and retested. Results, shown in Table II, indicate that chemical polishing does not significantly weaken specimens annealed at 2140°F(1170°C) or above. There did however appear to be a difference in fracture origins between the two types of specimens. As shown in Table III sanded specimens tended to have internal origins and chemically polished specimens surface origins, as was found in previous extensive testing of unannealed extruded specimens. Examination of the few surface grains that could be adequately viewed away from the fracture origin indicated a possible lower concentration of etch pits and slip bands than are found in surface grains of unannealed specimens. Amongst the internal fracture origins, a few more examples of slip bands at fracture were found. Some of these are shown in Figure 1.

(c) The Effect of Short Test Span on Bend Strength

Previous work had shown no effect of test span on strength in 3 point room temperature bend testing over the range 0.5" to 2.0" so long as only specimens failing at or near the center were considered. Further testing (see Table IV) shows the range can be extended down to 0.35" with reliable results.

(d) Longitudinal Fracture Strength

All previous testing of extruded MgO was with the tensile axis parallel to the axis of extrusion so the fracture was transverse (perpendicular to the extrusion axis). It was desired to test the strength at 90° to this, that is with the fracture parallel (longitudinal fracture) to the extrusion axis. Several specimens were obtained that were adequate for testing on a 0.35" span (typical extrusion

diameter is 0.5"). Results are plotted in Figure 2 showing that the average longitudinal fracture strength is lower than the average transverse fracture strength. In fact, the average longitudinal fracture strength appears to agree quite well with the average hot pressed (and fired) MgO strength. It was observed that two annealed extruded specimens from a hot pressed billet and one from a fused billet had about the same longitudinal fracture strengths for their grain sizes when chemically polished as the rest of the longitudinal fracture specimens tested as sanded (see Figure 2).

The longitudinal fractures were almost exclusively cleavage as with transverse fractures. Most origins of longitudinal fractures could not be determined nearly as well as for transverse fracturing. This appeared to be due to a more irregular fracture topography. However, the approximate region of origin could be determined for some specimens (Figure 3). Several of these origins from sanded specimens appeared to be internal (see Figure 3A) and there were some signs of slip bands in the regions of probable fracture origin. (Figures 3B, 4A). Occurrence of a higher surface density of dislocations and slip bands was also seen in the sanded specimens (Figure 4B).

(e) High Temperature Strength and Fracture

Preliminary strength data has been gathered by 3 point flexure at 2400°F (1315°C) using a platinum-rhodium resistance-heated furnace. Testing was on a 0.75" span using 0.10" diameter sapphire rod loading points. This data is plotted in Figure 5, along with data for several types of hot pressed MgO (see Appendix). The two extruded fused MgO specimens which appeared substantially stronger for their grain size failed mostly by cleavage which indicated origins at or near the surface (see Figure 6). The four extruded specimens from hot pressed (Fisher) MgO had about the same strength as the original hot pressed MgO of equivalent grain size. Three of these specimens had about 30-40% cleavage fracture near the tensile surface (see Figure 7) and 70-90% cleavage near the compression surface. This is substantially more cleavage than the hot pressed bodies. The partial intergranular fracturing prevented the determination of fracture origins. The fourth specimen, which was annealed at 2600°F(1425°C) prior to testing at 2400°F(1315°C), showed only 30-40% cleavage over the whole fracture surface.

3. MgO Pores and Impurities

As noted earlier, considerable intergranular fracture occurred at elevated temperatures. The exposed grain boundaries surfaces generally had round or elongated and curved objects on them as shown in Figure 7. Similar

objects are also seen on unextruded hot pressed MgO grain boundaries exposed by high temperature fracture. They have also been seen on grain boundaries occasionally exposed in room temperature fracture of as-extruded or annealed MgO bodies from hot pressed billets (Figure 8), and appear to be more common in the latter. Such intergranular fracture, and these objects, appears to be more common in room temperature testing of annealed extruded specimens, particularly in MgO-NiO bodies. These objects have not been observed on extruded fused MgO grain boundaries. Earlier, some of these objects on room temperature fractures were examined with an electron microscope and an electron probe. The objects always appear to be depressions, but appear to contain a smaller object (probably a protrusion) inside (see Figure 8A). Thus they appear to be pores containing a small protrusion. The probe showed no sign of impurities. (Note, the small protrusions are beyond the detectability of the probe.)

The occurrence of the above pores and a gray blue color in extruded Fisher MgO bodies suggested the presence of gas producing impurities, especially with only low temperature billet firing (see Appendix). IR transmission (Figure 9) clearly shows that most extruded specimens have absorption bands similar to those in hot pressed MgO (see Appendix), but shifted to longer wavelengths. Of eight extruded billets tested, five had bands such as that shown by specimens M-3-8 and -14 in Figure 9. Four of these were 1.5" diameter Fisher MgO billets fired to only 2200°F (1205°C)-2400°F (1315°C), and the fifth to only 2200°F (1205°C). The three not showing this band were: a 1.5" diameter Mallinckrodt MgO billet fired to 2900°F (1565°C), a 1.0" diameter Fisher MgO billet fired to 2400°F (1315°C), and a fused (mostly single crystal) MgO billet. (The smaller absorption bands at about 3.0 and 6.25 microns in the latter should not be weighed too strongly since this specimen was at least twice as thick as most of the other specimens).

4. Al_2O_3 Macrostructure

Further examination of the first Al_2O_3 extrusion revealed that the first billet (A-1-4: a 1" diameter piece of Coors AD-99 Al_2O_3) had extruded fairly uniformly (see Figure 10), and was white (and slightly translucent) in marked contrast to the high non-uniformity and gray color of the hot pressed Al_2O_3 and fused MgAl_2O_4 billets. The area reduction ratio was about 9 to 1 for both the Al_2O_3 and the cans. This extruded Al_2O_3 billet had transverse cracks spaced from about 0.1" to about 1.2" apart averaging about 0.5". Some limited longitudinal cracking was seen extending only a

short distance from the billet center. This Al_2O_3 extrusion was removed without difficulty from the can and showed no visible sign of contamination from the tungsten grit used inside the TZM can.

The second Al_2O_3 extrusion, containing only hot pressed Al_2O_3 and Al_2O_3 -1/2 w/o MgO was considerably more uniform than the first (previously reported), but still showed some metal protrusions into the Al_2O_3 (see Figure 11). Bubbles, as shown in Figure 11C, D, were observed fairly consistently throughout the center of the extrusion. The Al_2O_3 had area reduction ratios from about 15-40 to 1 in contrast to a can reduction of 9 to 1. All of the Al_2O_3 had a gray appearance.

5. Al_2O_3 Microstructure and Strength

The microstructure of the Al_2O_3 before and after extrusion is shown in Figure 12, indicating a reduction in grain size from about 13.5 to 9.5 microns. Both microstructures appeared to be fairly uniform. The extruded structure appears to be random indicating recrystallization (if the material properly extruded).

Strengths in Table V indicate 10 to 25% increases in room temperature strength in the extruded Al_2O_3 .

Two tests at $2400^\circ\text{F}(1315^\circ\text{C})$ of the extruded Al_2O_3 gave strengths of 8.03×10^3 psi and 8.10×10^3 psi. Both showed a slight bend-over at the end of the stress-strain curve.

II. DISCUSSION AND CONCLUSION

A. MgO

The occurrence of longitudinal cracking in extruded MgO without transverse cracking suggests different possible causes for the two types of cracking. This is further supported by the fact that longitudinal cracking found in extruded billets had considerable intergranular failure while transverse cracking was essentially all cleavage whereas both transverse and longitudinal room temperature fractures are essentially all cleavage. The occurrence of considerable intergranular fracture in longitudinal cracking of extrusions and the occurrence of such fracture in testing at $2400^\circ\text{F}(1315^\circ\text{C})$ suggests that longitudinal cracking of extrusions is occurring above $2400^\circ\text{F}(1315^\circ\text{C})$ in agreement with previous observations and estimates.

Previous results had shown that chemical polishing of as-extruded MgO specimens generally reduced strength. This was suggested to be due either to residual extrusion stresses (which were shown to exist) or to surface stresses

from work hardening surface grains (indicated by internal failures and higher surface dislocation and slip band densities). The close agreement of strengths of sanded specimens and chemically polished annealed specimens for either transverse or longitudinal fracture supports either of these two proposed postulates. The fact that annealed and, particularly, chemically polished specimens show more surface fracture origins indicates that work hardening of surface grains is occurring since these would allow removal of such hardening, thus favoring surface fracture origins.

The higher tensile strength of extruded MgO along the extrusion axis was concluded to be due to orientation which limited dislocation crack nucleation with supporting evidence from both strength and fracture data. An important prediction of this conclusion was that strength perpendicular to the extrusion axis should be lower, approaching that of random polycrystalline strengths. This is precisely what the data indicates, therefore lending considerable further support to the conclusion of dislocation crack nucleation in MgO. The scatter of the longitudinal strength data appears reasonable when it is recalled that flaws or weak areas will lower the strength of some specimens, while local orientation (probably from recrystallization of larger grains) could easily exist and result in some stronger longitudinal specimens.

Further evidence of both surface work hardening and dislocation fracture origins was presented.

Preliminary elevated temperature MgO strength data indicates that extruded hot pressed MgO has about the same strength but substantially more cleavage fracture than hot pressed specimens. However, these appear to have substantially less strength and cleavage than their companion extruded fused billets. The larger grain size of the latter does not appear adequate to explain their much greater cleavage fracture.

IR transmission clearly shows that many extrusions contain impurities which are probably carbonates (see Appendix). The greater occurrence of this impurity in Fisher MgO than in Mallinckrodt, in larger billets, and in lower fired billets is exactly as expected from the analysis of hot pressed bodies (Appendix). (Greater billet size would increase the occurrence of the carbonate because of the greater diffusion path for gas released from the center).

The data clearly indicate that the grain boundary objects in hot pressed billets are pores. These are believed to be caused by decomposition of the carbonate on cooling from extrusion, and increase on subsequent annealing or high temperature testing due to further decomposition in agreement with observations and study of hot pressed bodies (Appendix). The small objects in the pores may be the residue (e.g. MgO or CaO) from the decomposed impurity.

It is therefore suggested that the lower strength and cleavage of the extruded hot pressed bodies in comparison to extruded fused bodies is real and probably due to the porosity and residual gas producing impurity content of the former. It is difficult to tell whether the extruded MgO would have a clear advantage of strength at 2400°F(1315°C) in the absence of this porosity and gas producing impurity problem. However, the greater cleavage in the extruded hot pressed MgO over the hot pressed MgO indicates a change in fracture which in the absence of the above overriding problem might be associated with superior strength as it is at lower temperatures.

B. Al_2O_3

The greater uniformity of the first Al_2O_3 billet (Coors AD-99) in the first extrusion, the appropriate reduction ratio for the ceramic, and the reduction in its grain size indicate successful extrusion. These observations conflict with the previously reported suggestion of melting to explain the gross irregularity and apparent "squeezing to the back" of the rest of the Al_2O_3 and MgAl_2O_4 since the Coors AD-99 would be expected to melt lower than bodies from Linde A Al_2O_3 due to more impurities in the Coors alumina. However, melting may not yet be completely ruled out because:

- (1) Melting may have occurred in the hot pressed Linde A bodies due to heat from the greater work to extrude them since they are expected to be stiffer and harder than the commercial material (due to softening impurities in the latter).
- (2) The commercial fused MgAl_2O_4 at the rear may have melted (due to impurities and possible off-stoichiometry) and fluxed the adjacent hot pressed bodies.

The gray color of the Linde A bodies in both extrusions suggests possible reduction or contamination. However, the clean-white appearance of the Coors Al_2O_3 and the high chemical stability of Al_2O_3 in general would indicate reduction is unlikely.

The irregular nature of the cross sections, the much greater ceramic than can reduction, and the bubbles in the second extrusion also suggest melting, but the lower temperature of the extrusion and more uniform surface along the extruded Al_2O_3 contradict this suggestion.

One possible explanation that could agree with all the above observations is that gas producing impurities may have caused these problems. As shown in the Appendix, samples (about 1 gm) from hot pressed Linde A Al_2O_3 disks give off some H_2O , some sulfur or H_2S , and a fair amount of CO_2 . Large

billets could contain much more. It may be possible that such impurities cause the separation of grain boundaries due to released gas or by remaining as liquids in the parent phase under extrusion pressure so the material would behave like "lubricated-grit". This would probably cause non-uniformities similar to melting, but be more temperature dependent (due to more outgassing or lower viscosity at higher temperature) as observed. The center bubbles would be from unescaped gas (gas could escape from the surface since recently we have only tack welded tail plugs to allow for possible outgassing of billets). The large ceramic diameter at the rear of the first Al_2O_3 extrusion but not the second could be due to more flow of the softer "lubricated-grit" to the rear, melting of the MgAl_2O_4 , or less reduction of the MgAl_2O_4 due to possible greater stiffness. The large ceramic area reduction in the second extrusion could be due to extra space available from gas losses and particularly from densification of the Linde A "powder-billet" in the rear. The gray color of the extruded Linde A Al_2O_3 is the same as its hot pressed color which is believed due to gas producing impurities.

Thus, the anomalies of Al_2O_3 extrusion raise many questions, but the behavior of the Coors Al_2O_3 (though possibly aided by non-volatile impurities) appears to establish the extrudability of Al_2O_3 .

The strengthening of the extruded Coors Al_2O_3 may be due only to the slight reduction in grain size and slight densification. The low strength at elevated temperature is probably due to impurities such as SiO_2 , and the bend-over at the end of the stress-strain curve is probably only pseudo-ductility from grain boundary separation due to impurities (probably SiO_2). Further understanding of texture, strength, impurity, and surface finish relations must be established before conclusions can be drawn.

III. FUTURE WORK

The present extrusion difficulties (furnace failure and stalling) will be corrected and extrusions to explore changed MgO texture and mechanical properties of extruded MgO alloys will be carried out.

Further analysis of impurity effects in MgO , especially on high temperature properties, will be carried out. Placing a higher priority on MgO purification will be considered.

The problems of extruding uniform, solid Al_2O_3 pieces will be investigated. Particular emphasis will be placed on purer materials. To this end, use of sapphire crystals, high purity commercial aluminas (e.g. recrystallized Al_2O_3 and Lucalux), new powder sources, and improved processing of hot pressed bodies will be explored.

TABLE I

 Al_2O_3 EXTRUSION PARAMETERS

Extrusion No.	Can O.D. (in.)	Ceramic Billet Diameter (in.)	Temperature (1)	Area Reduction Ratio	Speed (in./sec)	Force (Tons)	
						(2) Upset	Running
Al_2O_3-1	3.5	1.0-1.5	1950°C	9 to 1	15	825	550
Al_2O_3-2	3.0	1.0-1.5	1850°C	9 to 1	6.7	600	600

(1) Temperature of composite can-ceramic billet on dropping from furnace.

(2) Force to extrude can metal nose.

TABLE II

SURFACE FINISH EFFECT ON STRENGTH OF EXTRUDED MgO

Specimens From Billet No.	Annealed at: then cut and tested:	Room Temperature Strength ¹ (Modulus of Rupture) in 1000 psi					
		2015°F(1100°C)		2140°F(1170°C)		2200°F(1205°C)	
		Sanded	Chemically Polished	Sanded	Chemically Polished	Sanded	Chemically Polished
M-1-16						19.8	21.9
M-3-3				35.5	34.0		
M-3-3				21.3 ^{2,3}	19.5 ²		
M-3-3				22.0 ^{2,3}	16.6 ²		
M-3-5				35.2	36.0		
M-3-5				31.6 ^{2,3}	29.9 ²		
M-3-5	30.8 ^{2,3}	17.9 ²					
M-3-14		24.0	37.0				

(1) Measured in 3 point bending with a 0.75" span unless otherwise noted. Head Travel: 0.05 in/min.

(2) Tested on a 0.35" span.

(3) Specimen exposed to atmosphere for several months after sanding before testing.

TABLE III
SURFACE FINISH EFFECT ON FRACTURE OF EXTRUDED MgO

Specimen Number	Fracture Origin of Annealed Specimens Tested:	
	As-Sanded	As Chemically Polished
M-3-14 _{1a}	Internal, 6 to 8 grains inside.	
M-3-14 _{1b}		At surface.
M-3-14 _{2a}	Internal, 2 to 3 grains inside.	
M-3-5 _{2-2a}	Internal, 2 to 5 grains inside.	
M-3-5 _{2-2b}		At surface.
M-3-5 _{1-2c}	Uncertain	
M-3-5 _{1-2b}		Internal, at 2nd grain inside.
M-3-5 _{1-3c}	Internal, at 2nd grain inside (see Figure 1).	
M-3-5 _{1-3b}		Origin at possible flaw at or near surface.
M-1-16 _{1a}	Internal, 3 to 6 grains inside.	
M-1-16 _{1b}		At surface.
M-3-3 _{2-2a}	Internal, 2nd grain inside.	
M-3-3 _{2-2b}		At surface.
M-3-3 _{1-1c}	Uncertain	
M-3-3 _{1-1b}		Uncertain
M-3-3 _{1-2c}	Uncertain	
M-3-3 _{1-2b}		Uncertain

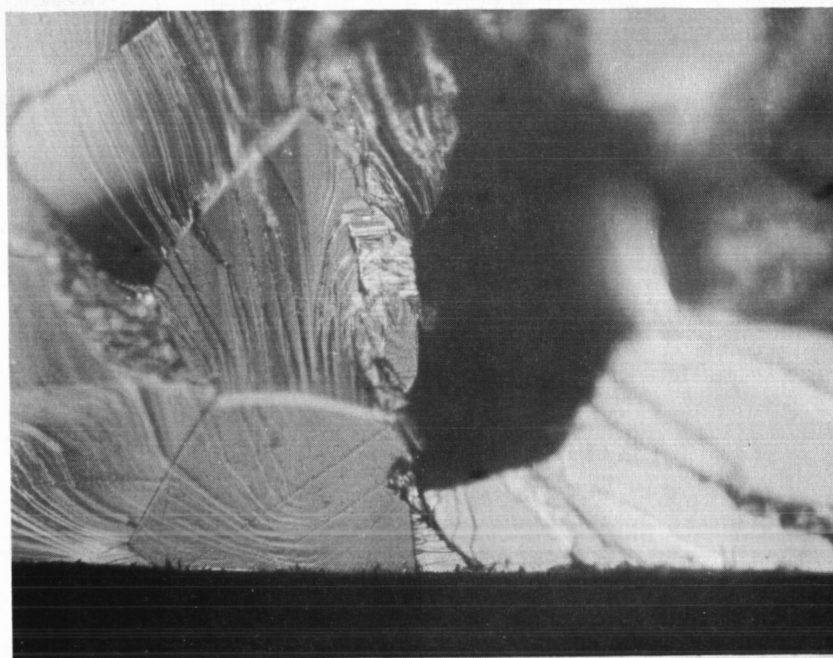
TABLE IV
EFFECT OF SHORT TEST SPANS ON EXTRUDED MgO TRANSVERSE BEND STRENGTH

Strength (Modulus of Rupture) in 1000 psi As Tested on Spans of:

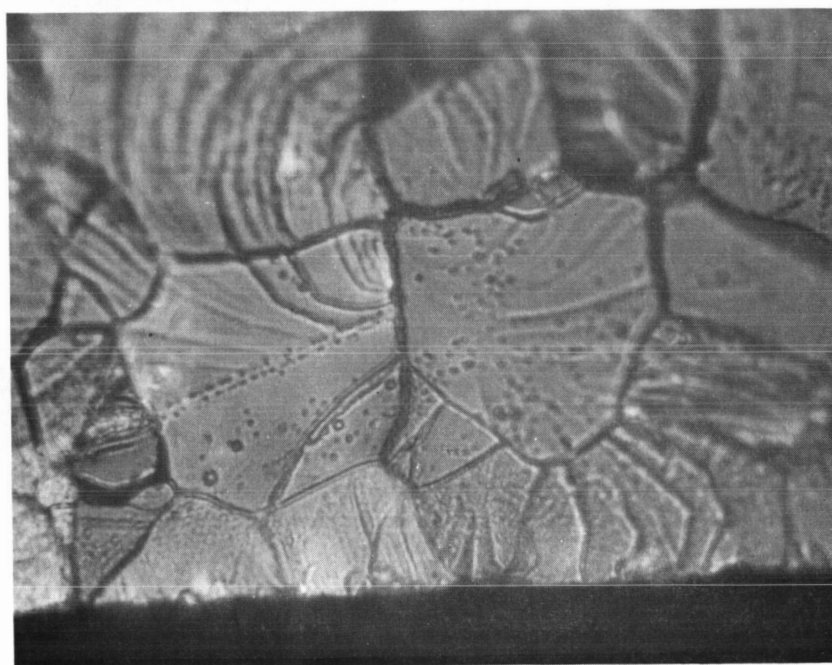
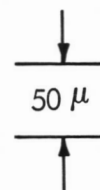
<u>Specimen Number</u>	<u>0.75"</u>	<u>0.50"</u>	<u>0.35"</u>
M-2-11		29.5	34.2
M-3-3 ₁₋₁	22.8		22.0
M-3-3 ₁₋₂	22.9		21.3
M-3-5 ₁₋₂	33.2		30.8
M-3-5 ₁₋₃			30.8
M2N-1-64		36.7	31.4
M2N-1-63		44.4	43.8

TABLE V
Al₂O₃ STRENGTH

	Room Temperature Strength in 1000 psi (Modulus of Rupture)
<hr/>	
Coor's AD-99:	
(1) As-Received - cut perpendicular to rod (starting billet) axis	39.1 40.7
(2) As-Received - cut parallel to rod (starting billet) axis	45.7 44.1
(3) Hot extruded - cut parallel to rod (starting billet) and extrusion axis	53.5 50.2 52.1



A



B

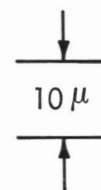


FIGURE 1 FURTHER EXAMPLES OF SLIP BANDS AT TRANSVERSE FRACTURE ORIGINS (A) Specimen M-f-9 1-1_c (B) Specimen M-3-5 1-3_c

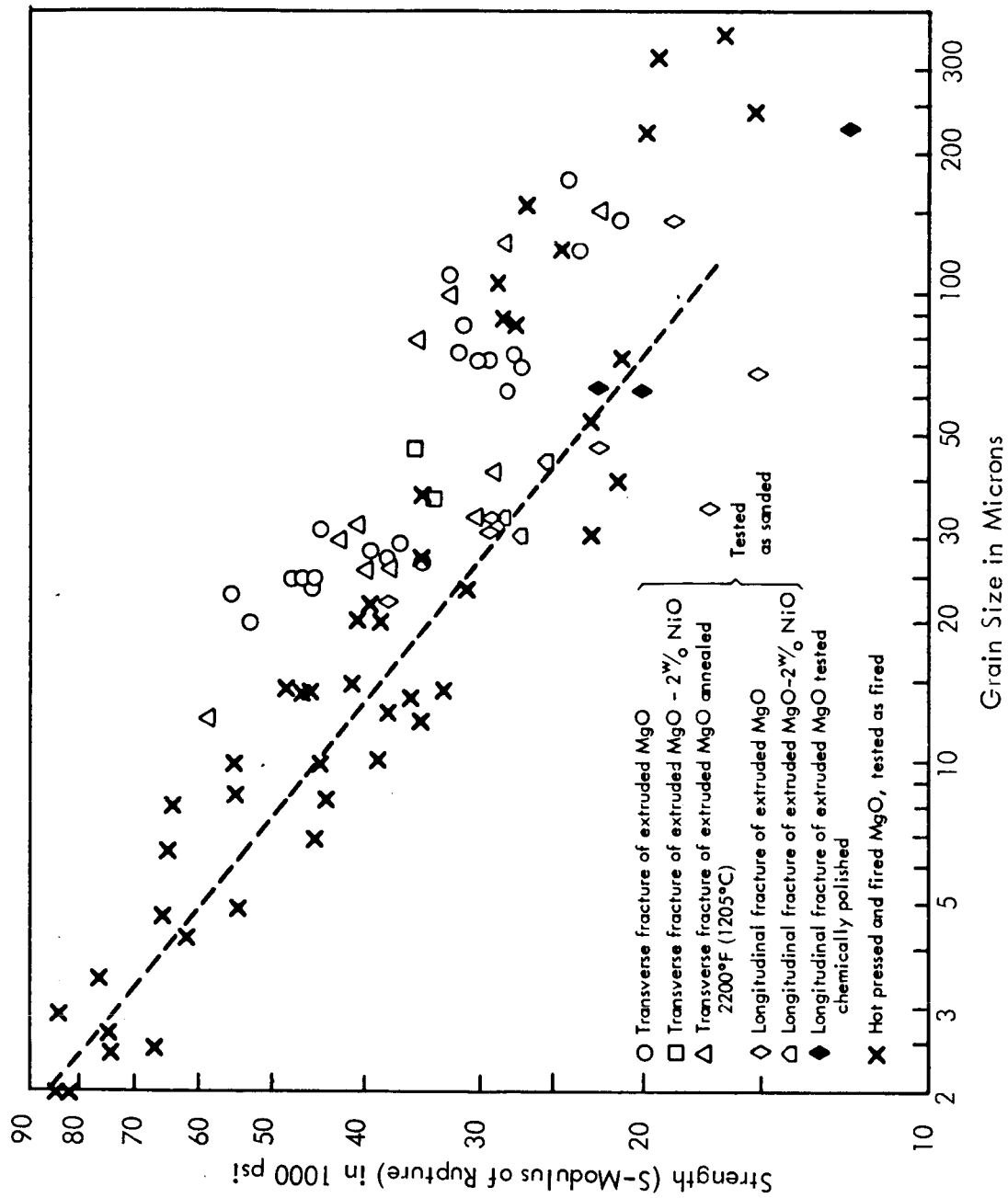
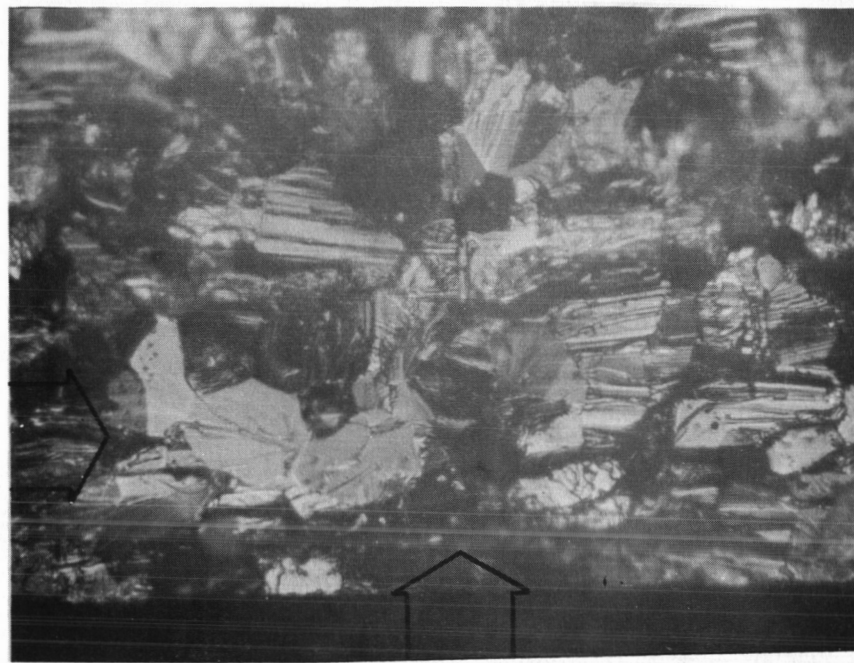


FIGURE 2 - ROOM TEMPERATURE STRENGTH OF EXTRUDED MgO

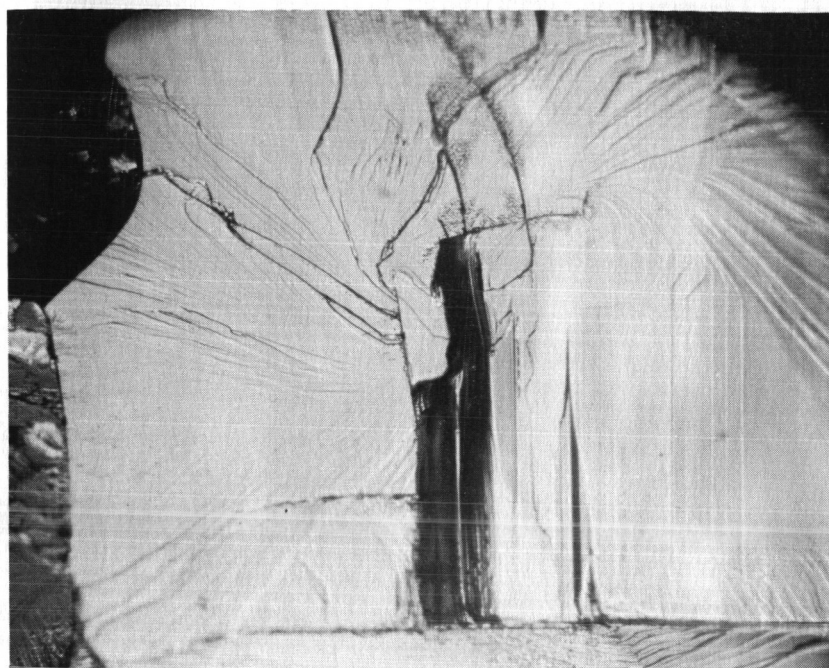


A



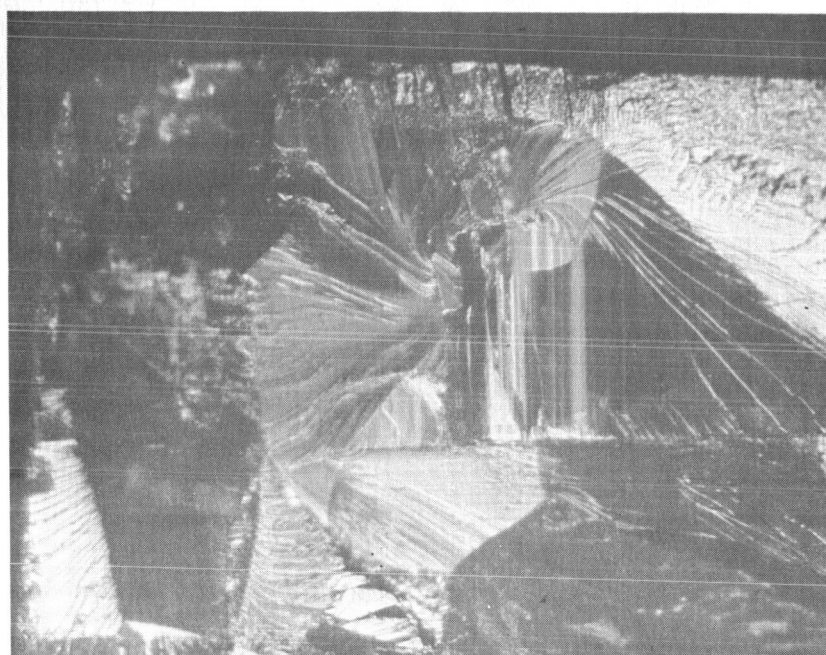
B

FIGURE 3 SAMPLE LONGITUDINAL FRACTURES (A) Specimen M-3-7 I_{1-1} Clearer than average fracture origin - inside specimen, (B) Specimen M-f-3 I_{1-1} clearer than average fracture origin - at surface or in 1st grain



D

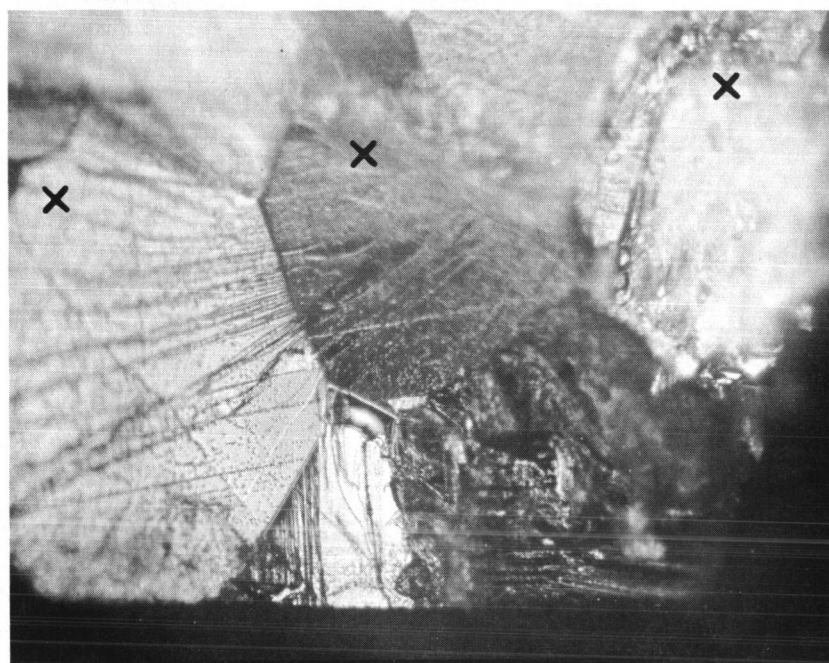
100 μ



C

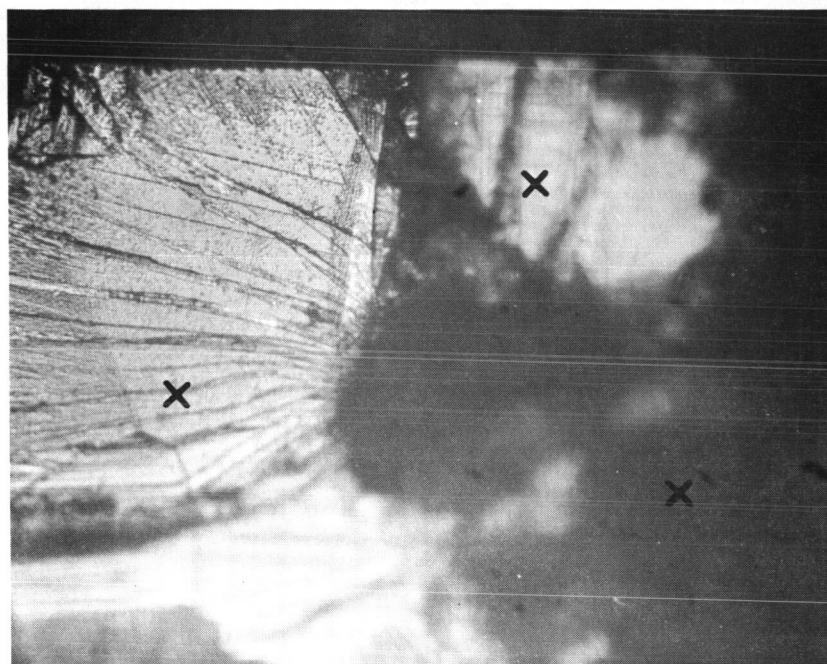
50 μ

FIGURE 3 SAMPLE LONGITUDINAL FRACTURES (Cont.)
 (C) Specimen M-f-3 1-2, definite internal origin, (D) Higher magnification of (C) etched



A

50 μ



B

100 μ

FIGURE 4 LONGITUDINAL FRACTURE ORIGIN AREA OF M-f-3I₁₋₁ (A) Etched half showing slip bands in grain near origin, grains with slip bands marked with X, (B) Etched matching half showing higher surface density of slip bands, Other grains with higher density are marked with X

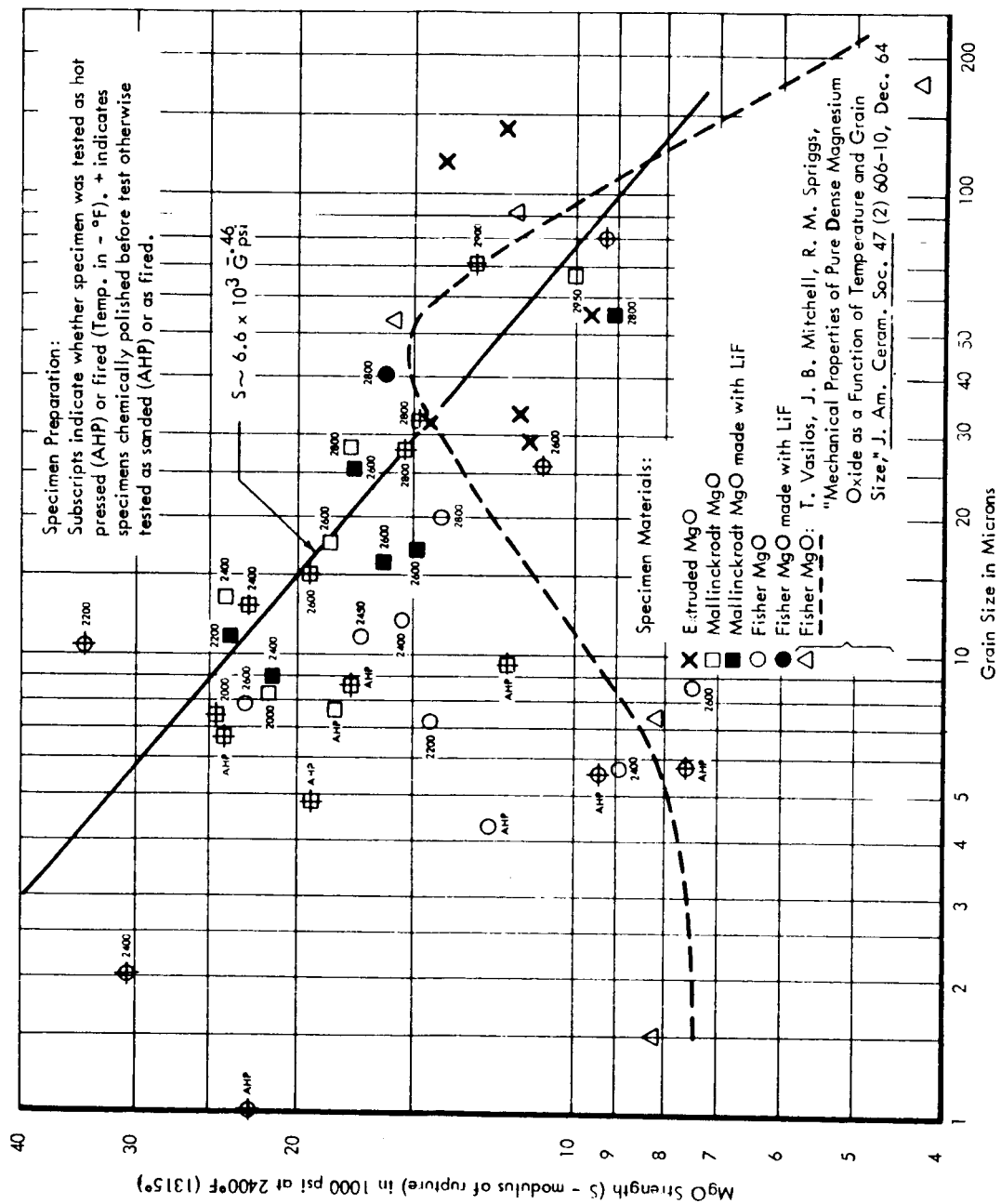


FIGURE 5 - 2400°F (1315°C) MgO STRENGTH

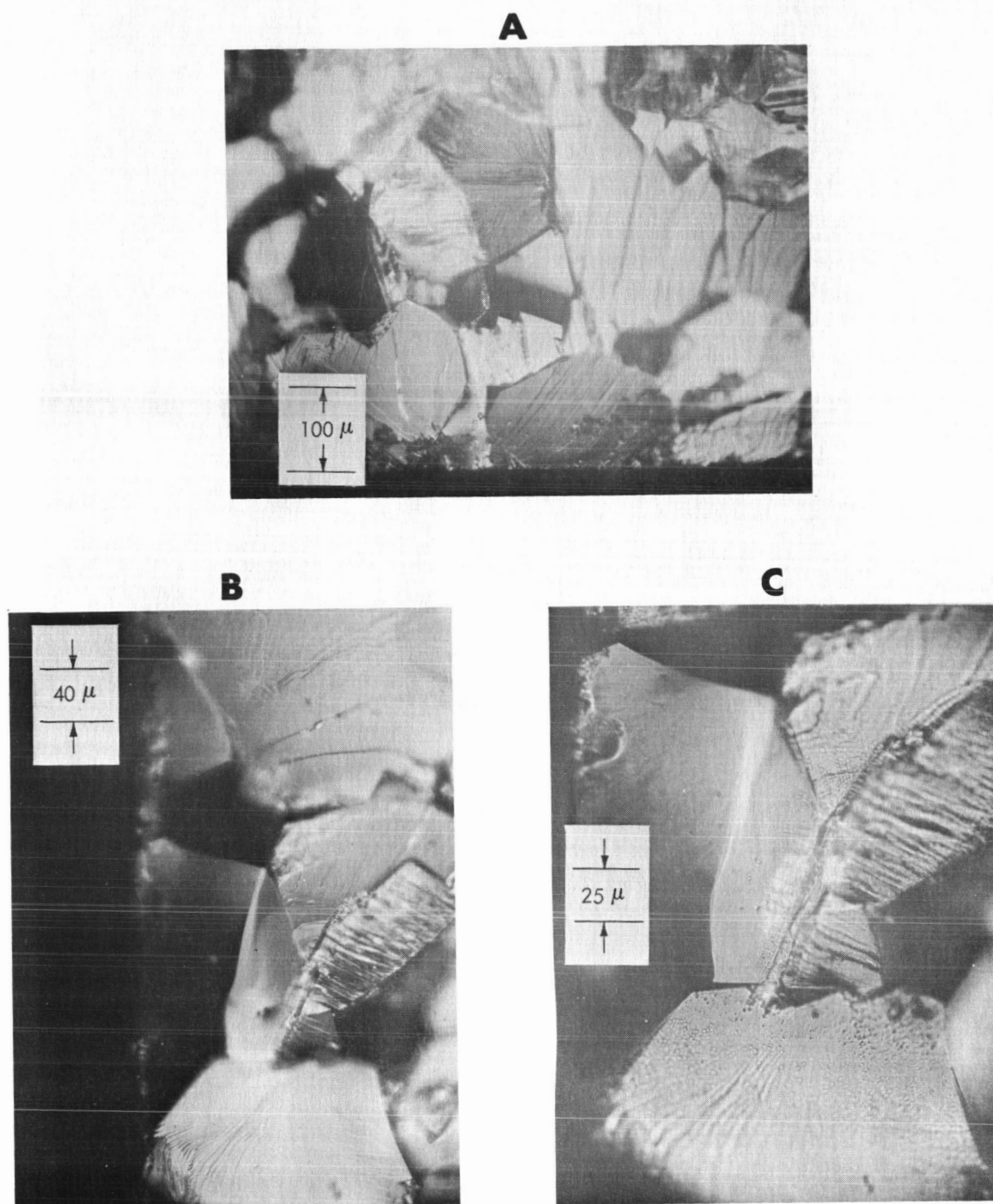
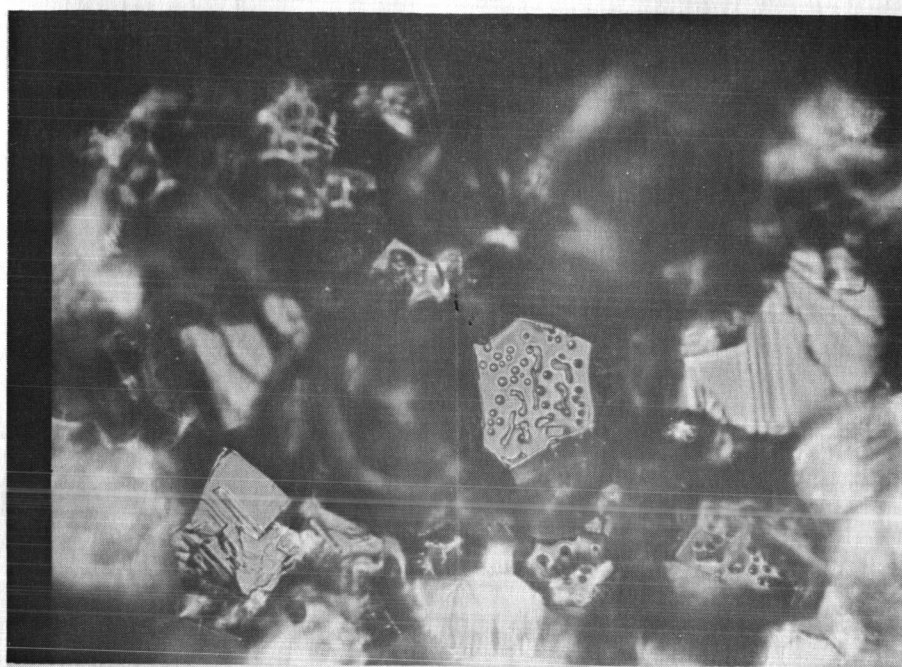


FIGURE 6 FRACTURE ORIGINS OF EXTRUDED FUSED SPECIMENS TESTED AT 2400°F (1315°C) (A) Specimen M-f-2 1-1, (B) Specimen M-f-9 1-1_a, (C) Specimen M-f-9 1-1_a etched



A

—| 20 μ |—



B

FIGURE 7 - 2400°F (1315°C) FRACTURE SURFACES OF EXTRUDED HOT
PRESSED MgO (A) M-3-52-2C, (B) M-3-18₁-4

Note: Objects on grain boundary surfaces

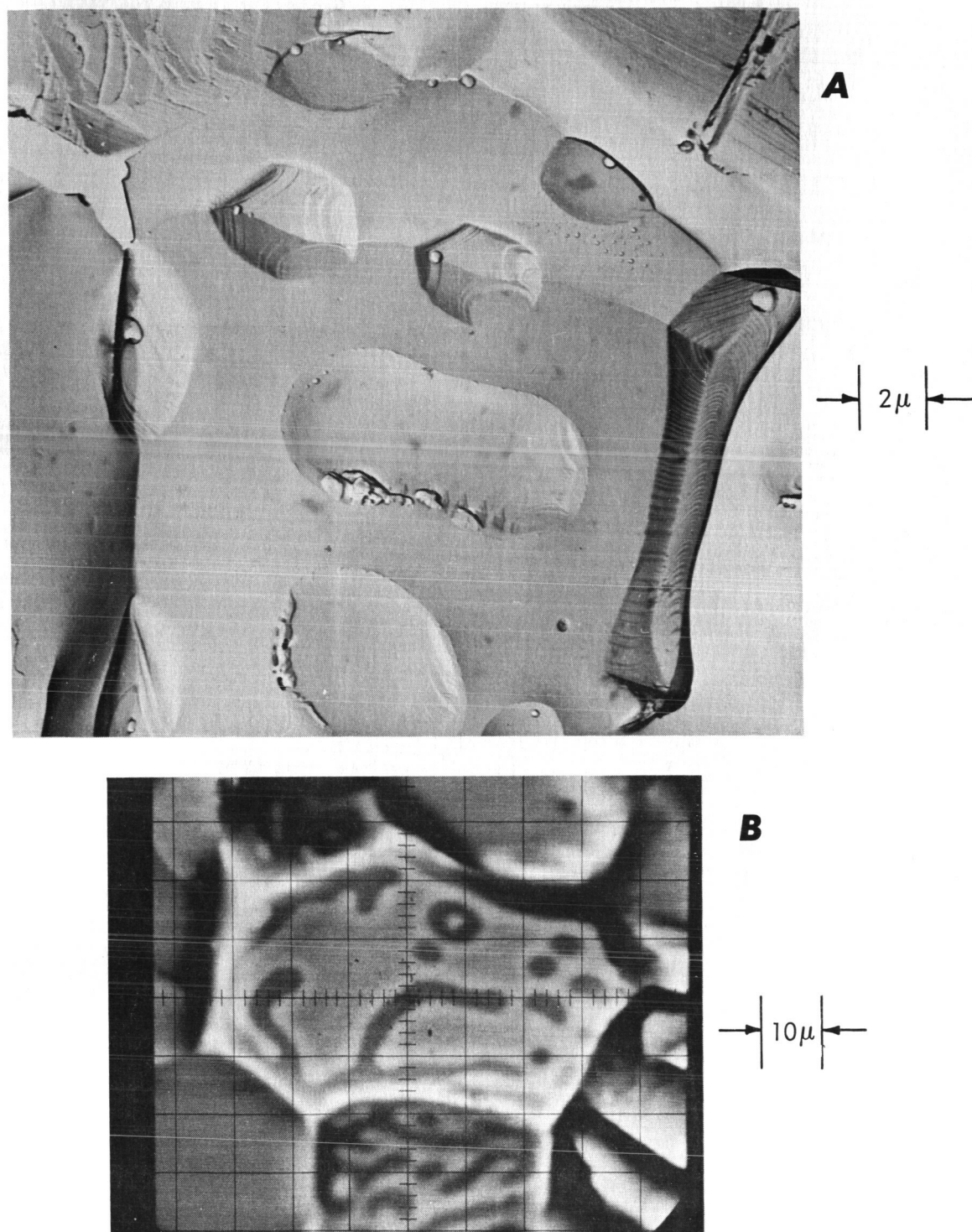


FIGURE 8 - OBJECTS ON EXTRUDED MgO GRAIN BOUNDARY SURFACES
 (A) Electron micrograph of specimen M-3-18_{1-3C}, Note shadowing indicating these are indentations. Also note smaller objects within larger objects, (B) Electron probe (specimen current) photo from same specimen, but different area (fracture origin)

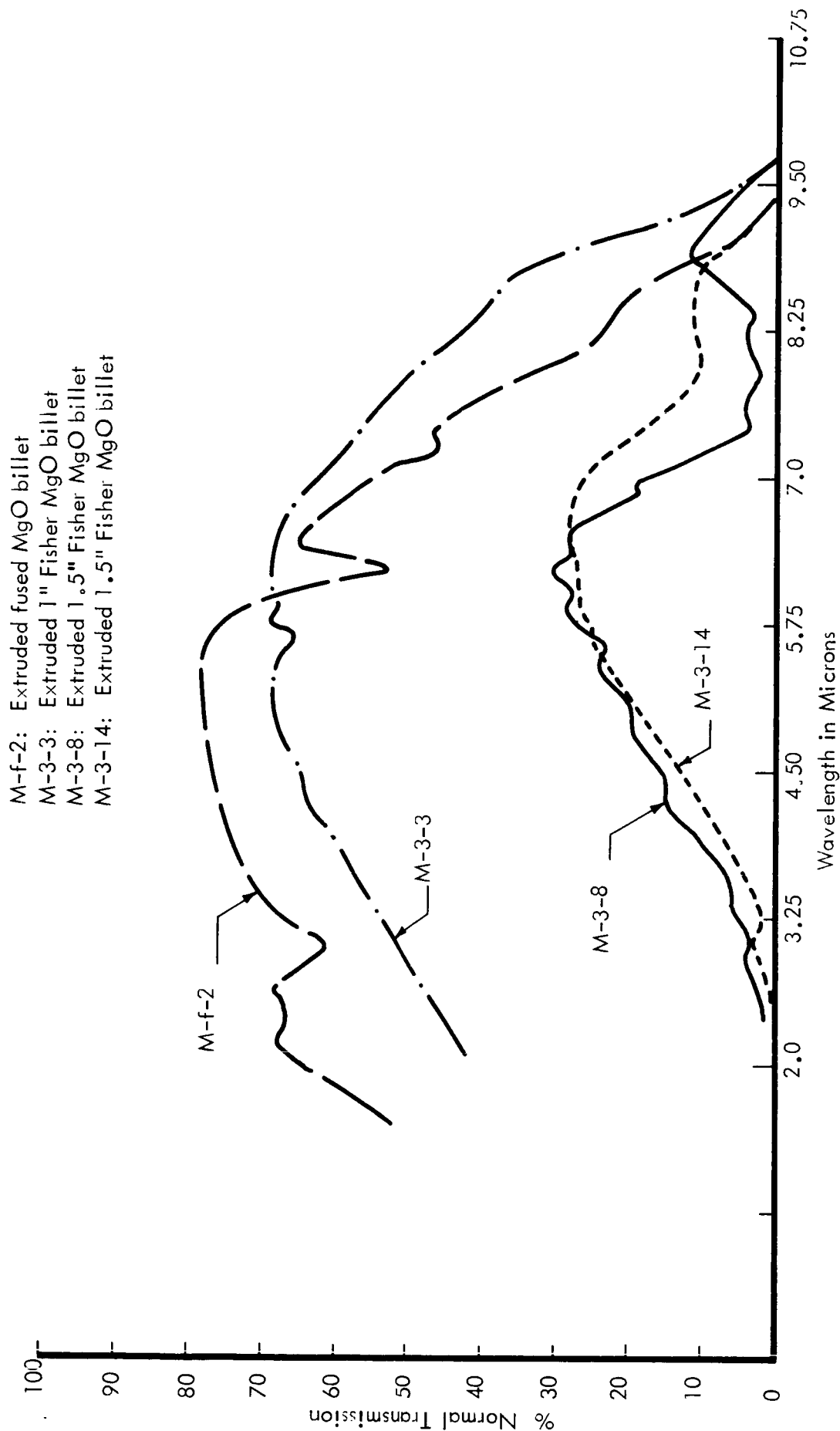


FIGURE 9 - I.R. TRANSMISSION OF EXTRUDED MgO
 Specimen Thickness 0.050" - 0.110"

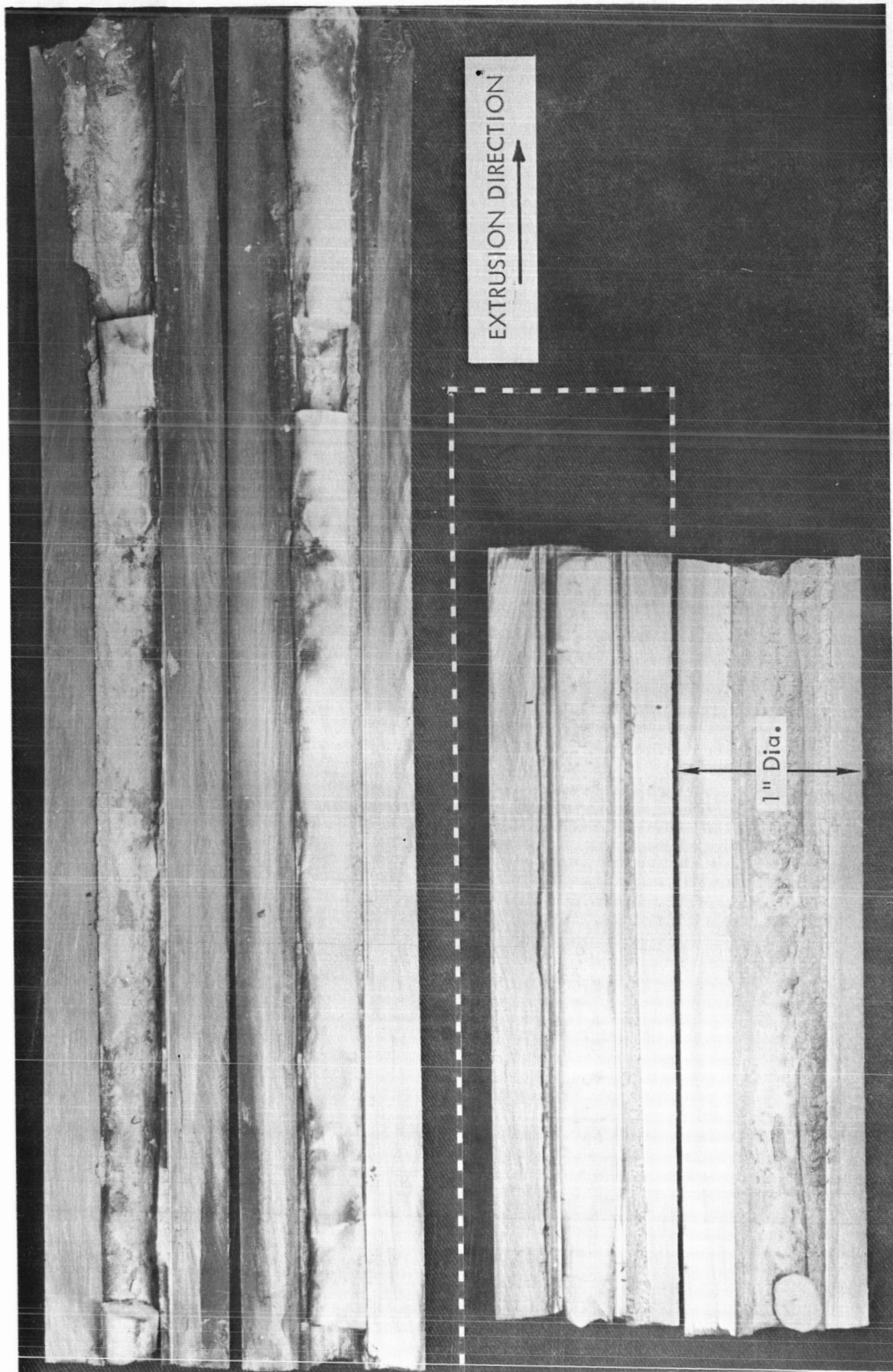
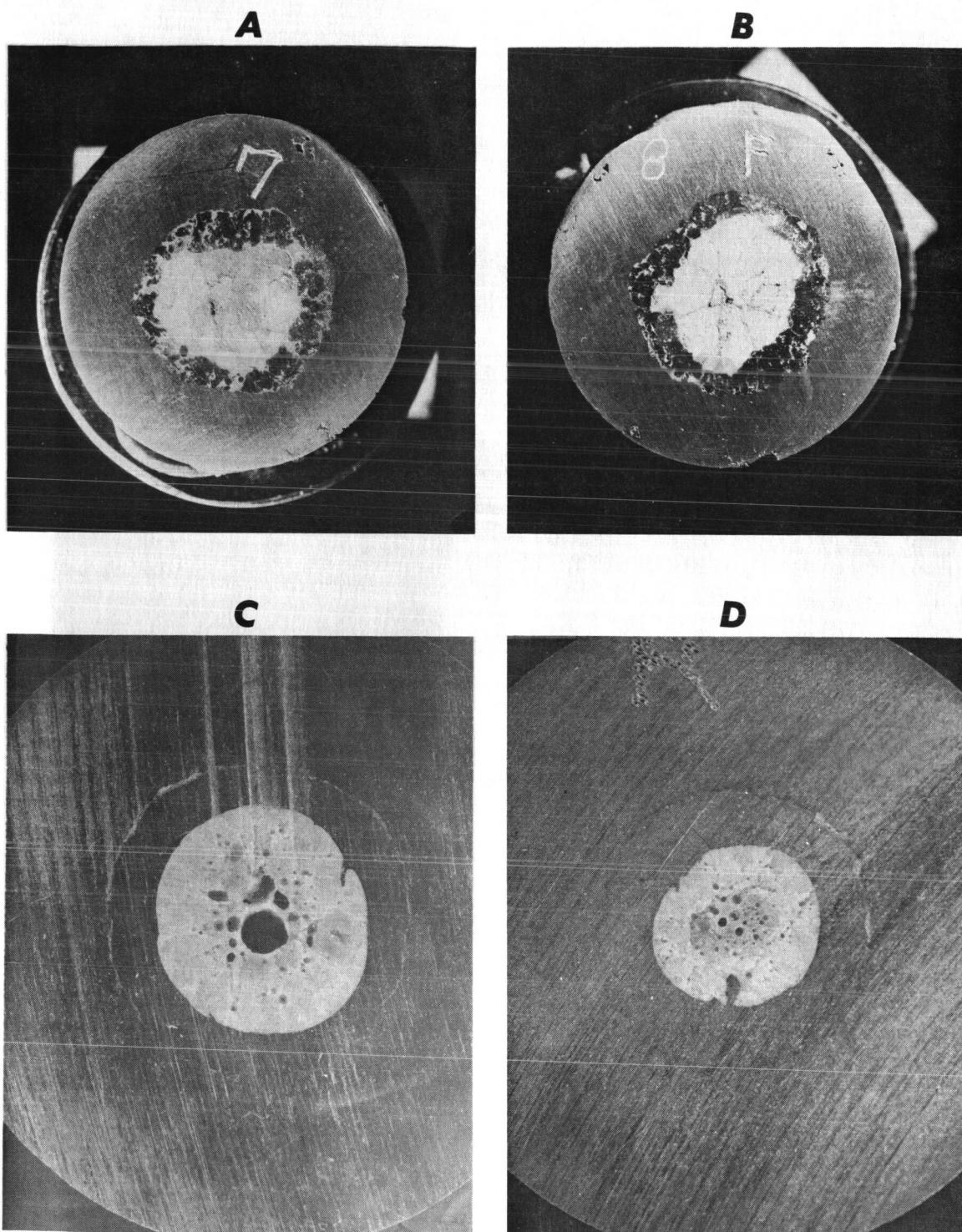
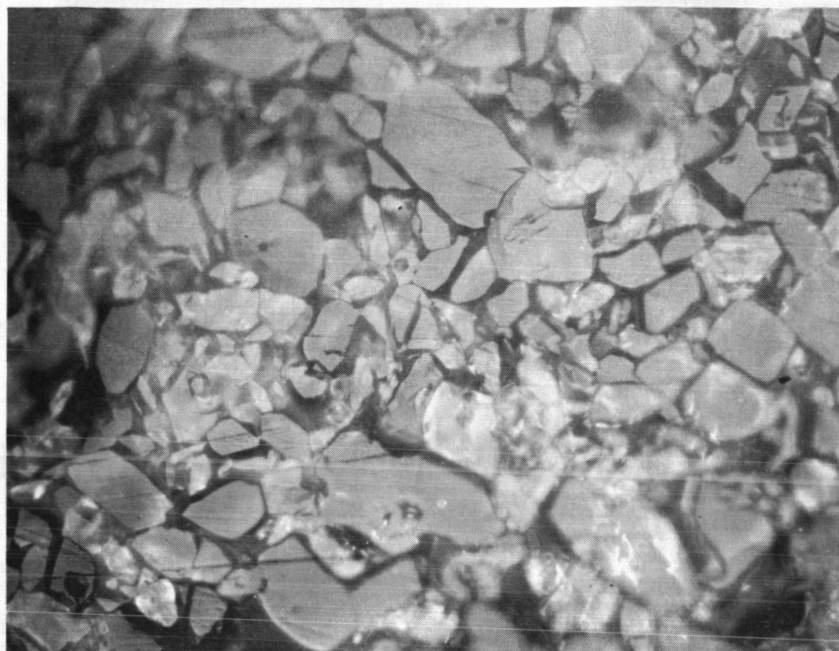


FIGURE 10 EXTRUDED Al_2O_3 BILLET A-1-4 IN CAN



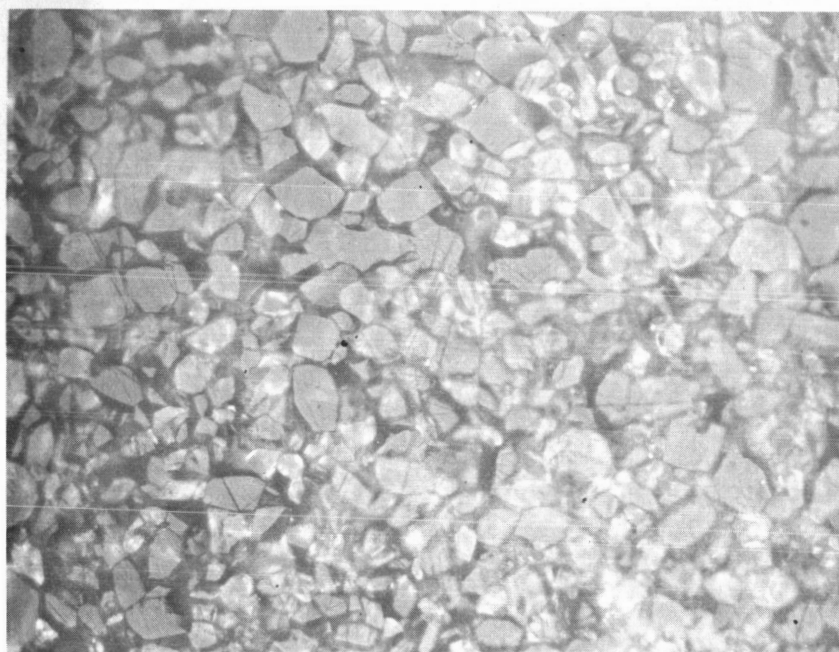
Note: Can Dia. $\approx 1''$

FIGURE 11 SAMPLE EXTRUDED Al_2O_3 CROSS SECTIONS
(A), (B) Extrusion Al_2O_3 -1 (C), (D) Extrusion Al_2O_3 -2



A

→ 20μ ←



B

FIGURE 12 - MICROSTRUCTURE OF Al_2O_3 BILLET A-1-4 (COORS AD 99)
(A) Before Extrusion, (B) After Extrusion (longitudinal section)

APPENDIX

GAS-PRODUCING CONTAMINANTS IN MgO AND Al_2O_3 AND THE HIGH TEMPERATURE PROPERTIES OF MgO

Gas-producing contaminants can be trapped in MgO ^(1, 2, 3) and Al_2O_3 ⁽³⁾ by hot pressing. In MgO , these contaminants can readily be detected by absorption bands in IR transmission through fairly translucent hot pressed samples. Typical IR transmission curves for hot pressed MgO (Figure 1) show a distinct absorption band at about 7 microns for bodies made from either Mallinckrodt or Fisher Reagent MgO with or without additives such as LiF . This same band is also observed for some MgO bodies made from calcined magnesium hydroxides and basic carbonates. Specimens fabricated at lower temperature (with LiF or NaF) sometimes show bands at about 2.8 and 4.0 microns.

Single crystals of $\text{Li}(\text{OH})_2$ ⁽⁴⁾, $\text{Mg}(\text{OH})_2$ ⁽⁵⁾ and $\text{Ca}(\text{OH})_2$ ⁽⁶⁾ all show several IR absorption peaks between 2.5 and 3.1 microns whose relative intensities depend on crystal orientation. It appears reasonable to assume that the combined effect of these in a polycrystalline body would be an absorption band at about 2.8 microns. Magnesium basic carbonate shows such a band⁽⁷⁾.

Alkali bicarbonates^(7,8) have an absorption band at about 4 microns.

Many carbonates, including magnesium and calcium, have a strong absorption band at 7 microns⁽⁷⁾, and magnesium basic carbonate and Li_2CO_3 have a double peaked band with a peak at about 7 microns and one at about 6.6 microns.

Thus, it is concluded that hot pressed MgO has carbonates trapped in it and that if fabricated at lower temperatures (about 1000°C) it may also have hydroxides and bicarbonates. These are most likely magnesium compounds, but could also be those of impurities such as calcium.

Firing of hot pressed bodies removes the gaseous impurities as shown directly by infrared transmission and mass spectrometry. It is also shown indirectly by measureable weight losses, clouding, bloating, and blistering of specimens. The latter problems occur if the body is either fired too fast or has too much of the above gas producing impurities. Infrared transmission indicates that temperatures of about 1100°C or less are adequate to remove absorption bands attributed to hydroxides and bicarbonates from specimens about 0.1" thick. Removal of the band attributed to carbonate is very dependent on material source. Mallinckrodt MgO specimens (about 0.1" thick) lose this carbonate absorption band after firing to temperatures of only about 1100°C or less, while similar specimens made from Fisher MgO require temperatures of 1600°C or more. These results appear to be independent of whether or not an additive such as LiF was used.

Mass spectrometer data (using a Knudsen Cell) in Figure 2 shows the difficulty of removing both H_2O and CO_2 from dense, hot pressed Fisher MgO since both the as-hot-pressed and fired (about 1200°C) sections from the same pressing show H_2O and CO_2 coming off at temperatures up to about 2100°C and over 2200°C respectively. The substantial reduction of such outgassing after firing to 3100°C is in agreement with the IR results. The greater amount of water indicated in Figure 2B over 2A is probably due in part to variations within a hot pressed disk. The presence of water in the mass spectrometer test is not in conflict with the IR data since the latter is less sensitive. (It also appears that the IR is less sensitive for OH as compared with CO_3 detection.) These H_2O results are in agreement with results of Neilsen and Leipold⁽⁹⁾.

Rice^(2,3) has shown that a maximum of strength occurs in Fisher MgO after slow firing to temperatures of about 2200°F (1205°C) with some variation from sample to sample. It has been suggested that part of this initial increase in strength may be due to removal of some gaseous impurities, at least from the surface (since this would be most significant in bend testing). The above data showing a maximum of H_2O outgassing in the 800 – 1200°C range (on a faster firing cycle) would appear to agree with this observation.

Strength versus grain size for MgO at 2400°F (1315°C) is shown in Figure 3. Again, the fine grain specimens which have not been fired to very high temperatures and therefore have more gas producing impurities, are weaker than specimens fired to somewhat higher temperatures prior to testing. This is particularly pronounced for Fisher MgO which retains the most gas producing impurity to the highest temperature. It is believed that the greater amount of gases are responsible for the reduction in strength at fine grain sizes due to internal stresses from decomposition within the body. Preliminary comparison shows that the strongest specimens in a given grain size range generally have the weaker IR absorption bands. High temperature fractures are almost exclusively intergranular. This may be due in part to such gases collecting or forming at grain boundaries, thus aiding boundary separation. Using only the stronger specimens (i.e., the ones apparently least compromised by these impurities) a straight line relationship of strength, $S \sim 6.6 \times 10^3 G^{.46}$ psi, to grain size is obtained. This is in very good agreement with reported room temperature grain size functions⁽³⁾.

Al_2O_3 , though less extensively investigated to date, appears to present some of the same gas problems as MgO . Figure 4, data of a mass spectrometer run of a hot pressed Linde A Al_2O_3 body, shows some outgassing, though less than for MgO . This data indicates an additional species of mass number 34 which is believed to be H_2S . This is feasible since the starting powder is derived from a sulfate and shows much greater mass 34 outgassing (the H_2S could be formed in the time of flight mass spectrometer tube from sulfur or a sulfurous ion and water). Residual sulfate could be converted to sulfide in graphite dies. Analysis is more limited since the IR cut off of Al_2O_3 makes analysis for SO_3 and CO_3 more difficult. These results are in agreement with several other observations: the vacuum hot press has a strong "sulfur smell" after pressing Al_2O_3 , especially at higher temperatures, and in some such high temperature pressings, a fine yellow-brown dust has been found on the top die ram. Dense, hot pressed Al_2O_3

is gray to blue in color, not white, and this color is not "burned out" until temperatures much higher than expected for graphite contamination. There are indications of a weight loss in Al_2O_3 upon firing, though much less than in MgO . There are also indications of initial slow firing resulting in less decrease in strength or even increases, but control of surface condition makes interpretation very uncertain at this time. Fracture surfaces have some suggestion of a second phase on grain boundary surfaces.

The lower gas content of Linde A Al_2O_3 compared to MgO could be due in part to its much larger particle size (about 0.5 micron compared to about 0.05 micron). Linde B Al_2O_3 , a much finer powder may contain more gas producing impurities, which could be in part responsible for the generally lower strength of dense bodies made from Linde B compared to equivalent Linde A bodies. Linde B also sometimes produces bodies with a black core and a quite translucent outside layer, quite the opposite that would occur if graphite contamination or reduction was the cause of this. The translucent areas cloud on firing, and the black requires temperatures over 1400°C for complete removal from bodies about 0.06" thick.

The lower amount of outgassing from Al_2O_3 and less established correlation of this with other changes in such bodies makes correlation of high temperature strength quite speculative at this point. However, the only pure Al_2O_3 body showing very definite macroscopic ductility at 2400°F (1315°C) at Boeing to date was hot pressed at lower temperatures, higher pressures, and shorter time than normally used (all favorable for greater retention of gas producing impurities). Grain size was about 0.5 micron. All other bodies, in particular all fired bodies (hence likely to have much smaller gas-producing impurity contents) were completely brittle though some had grain sizes of 1 micron or less. Some signs of limited local grain boundary sliding are seen in some of these specimens. This suggests that such gas producing impurities may aid grain boundary sliding to produce a pseudo-ductility. Such effects could be particularly pronounced at low strain rates or in creep testing.

APPENDIX

Note: (LiF) means that the specimen was hot pressed with LiF

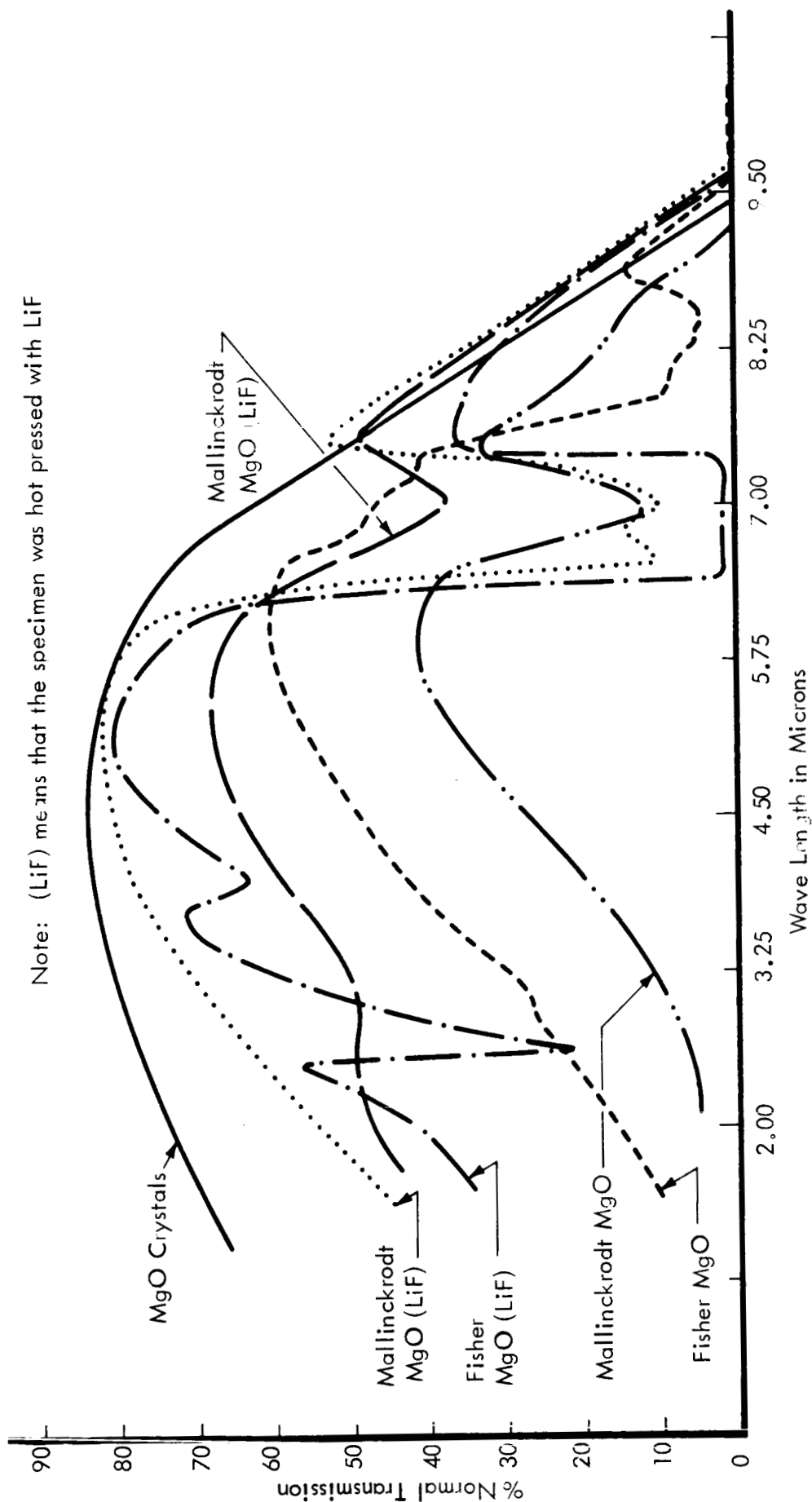


FIGURE 1 - TYPICAL I.R. TRANSMISSION OF AS-HOT-PRESSED MgO

APPENDIX

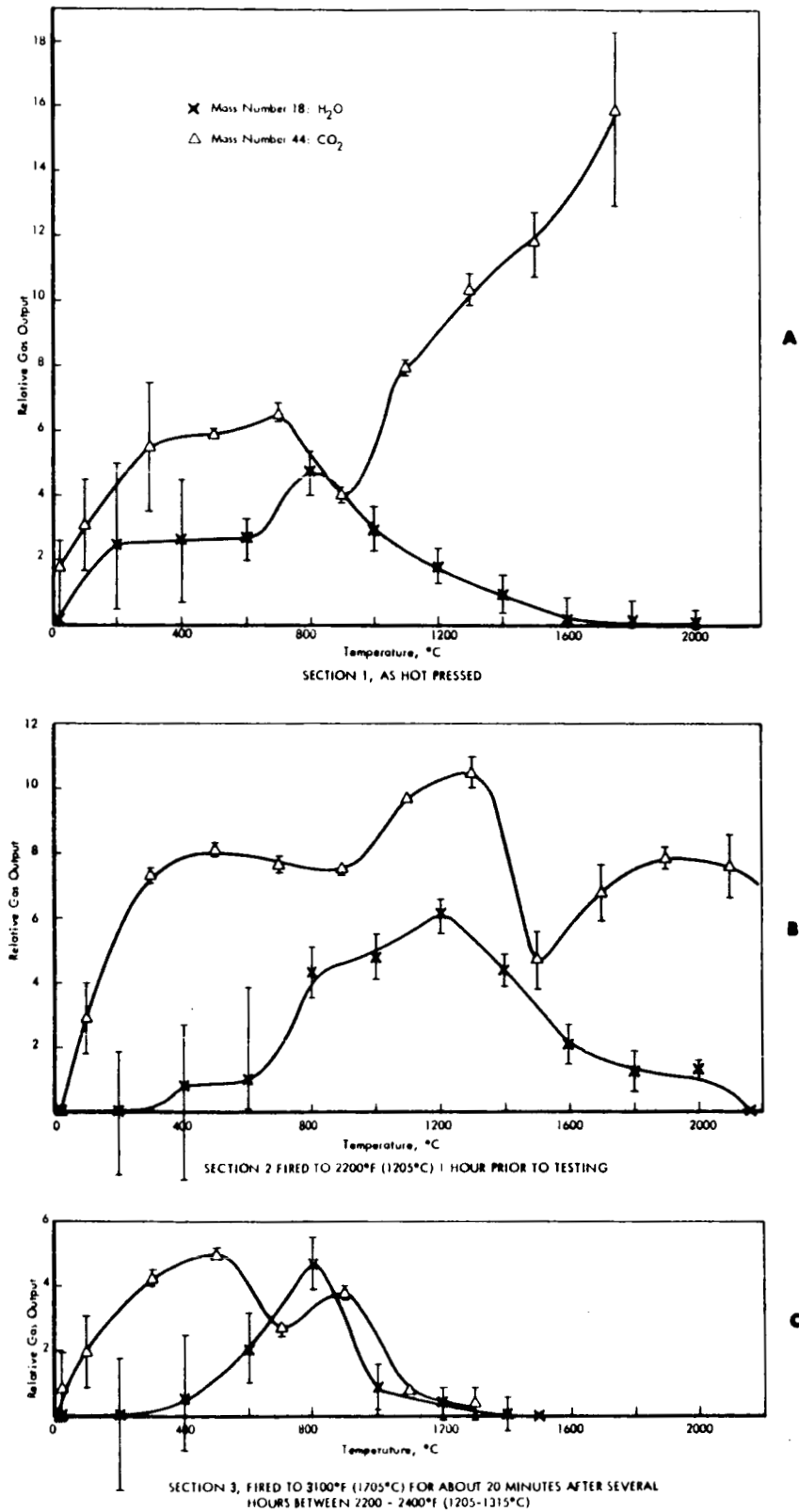


FIGURE 2 - MASS SPECTROMETER DATA FOR HOT PRESSED FISHER MgO

APPENDIX

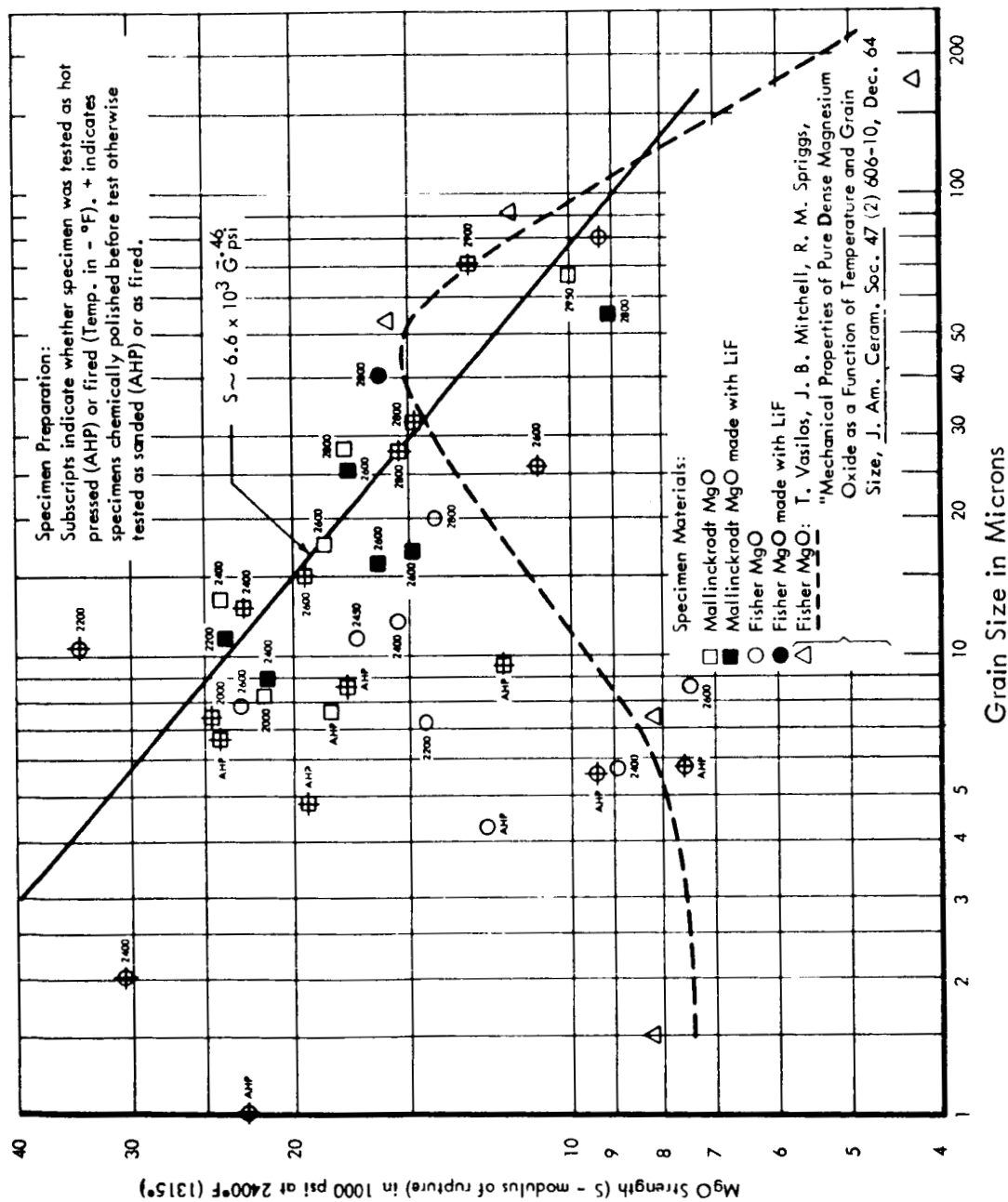


FIGURE 3 - MgO STRENGTH AT 2400°F (1315°C)

APPENDIX

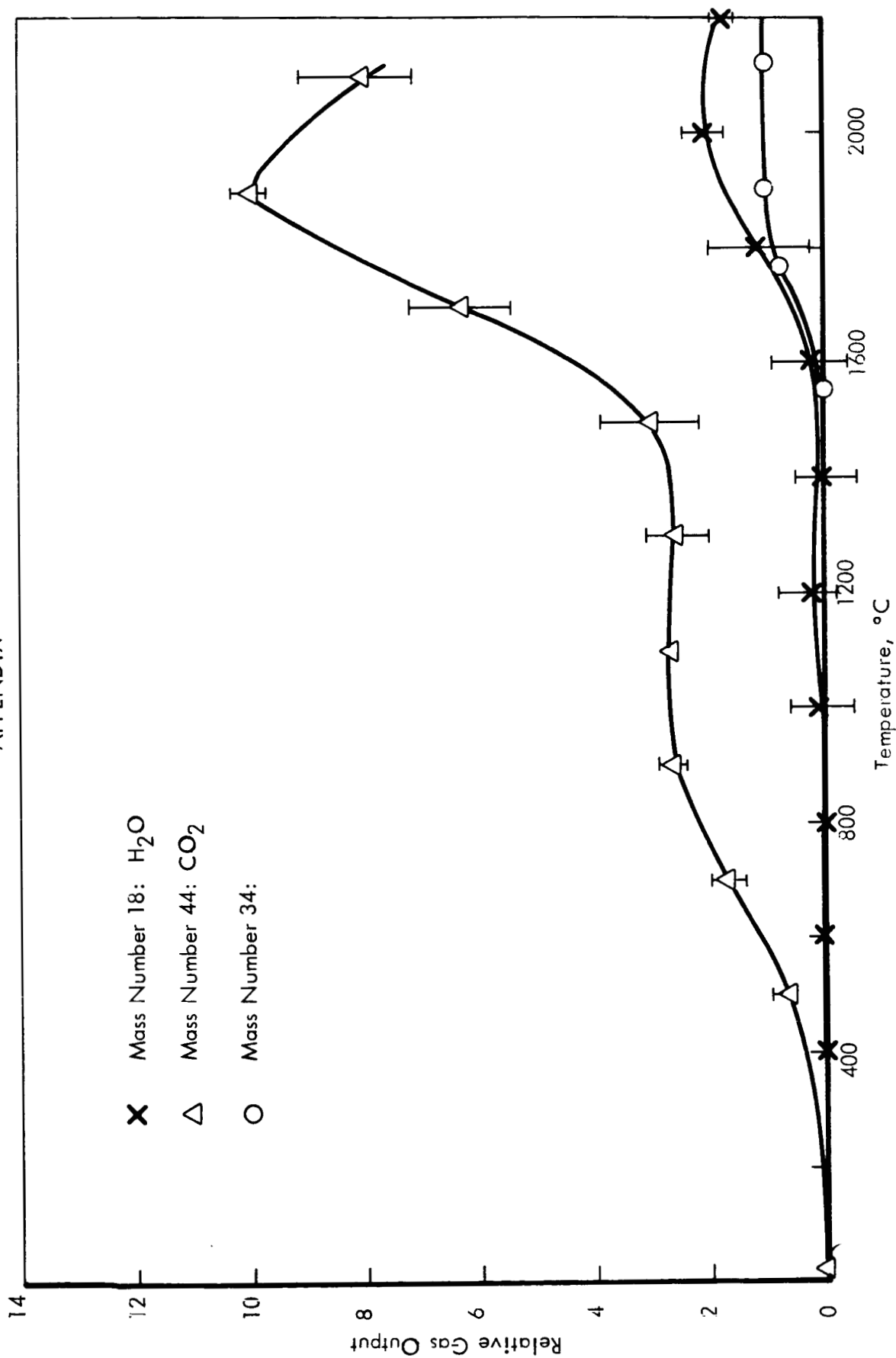


FIGURE 4 - MASS SPECTROMETER DATA FOR HOT PRESSED
LINDE A Al₂O₃

APPENDIX REFERENCES

1. R. W. Rice, "Production of Transparent MgO at Moderate Temperatures and Pressures", Presented at the 64th Annual Meeting of the American Ceramic Society in New York, N.Y., May 1962 (Abstract: Am. Ceram. Soc. Bul 41 (4) p. 271, April 1962).
2. R. W. Rice, "Internal Surfaces in MgO", Materials Science Research Vol. 3: The Role of Grain Boundaries and Surfaces in Ceramics (Ed. by W.W. Kriegel and H. Palmour III), Plenum Press, New York, N.Y. (1966).
3. R. W. Rice, "Strength and Fracture of Dense MgO", Presented at the 3rd International Symposium on Materials: Ceramic Microstructures - Their Analysis, Significance, and Production, June 1962 in Berkeley, Calif. (Proceedings to be published by Wylie Press).
4. K. A. Wickersheim, "Infrared Absorption-Spectrum of Lithium Hydroxide", J. Chem. Phys. 31 (4), p. 863-69, October 1959.
5. R. T. Mara, G. B.B.M. Sutherland, "The Infrared Spectrum of Bruate $\text{Mg}(\text{OH})_2$ ", J. Opt. Soc. Am. 44, pp 1100-2, 1953.
6. W. R. Busing; H. W. Morgan, "Infrared Spectrum of $\text{Ca}(\text{OH})_2$ ", J. Chem. Phy 28 (5) p. 998-99, May 1958.
7. F. A. Miller, C. H. Wilkins, "Infrared Spectra and Characteristic Frequencies of Inorganic Ions", Anal. Chem. 24 (48), p. 1253, August 1952.
8. L. C. Afremow, J. T. Vandenberg, "High Resolution Spectra of Inorganic Pigments and Extenders in the Mid-Infrared Region from 1500 cm^{-1} to 200 cm^{-1} ", J. Paint Tech. 38 (495), pp. 169-202, April 1966.
9. T. H. Nielsen, M. H. Leipold, "Surface Adsorption in Magnesium Oxide", Technical Report 32-949, Jet Propulsion Laboratory, June 1966.